Institute for
Shock Physics
Washington State University

"Complete Equation of State for Shocked Liquid Nitrogen: Analytical Developments"

J. M. Winey and Y. M. Gupta

Accepted Date: July 2016

Journal of Chemical Physics

Complete Equation of State for Shocked Liquid Nitrogen: Analytical Developments

J. M. Winey and Y. M. Gupta

Institute for Shock Physics and Department of Physics, Washington State University, Pullman WA 99164-2816

Abstract

The thermodynamic response of liquid nitrogen has been studied extensively, in part, due to the long-standing interest in the high pressure and high temperature dissociation of shocked molecular nitrogen. Previous equation of state (EOS) developments regarding shocked liquid nitrogen have focused mainly on the use of intermolecular pair potentials in atomistic calculations. Here, we present EOS developments for liquid nitrogen, incorporating analytical models, for use in continuum calculations of the shock compression response. The analytical models, together with available Hugoniot data, were used to extrapolate a low pressure reference EOS for molecular nitrogen [Span, *et al.*, J. Phys. Chem. Ref. Data **29**, 1361 (2000)] to high pressures and high temperatures. Using the EOS presented here, the calculated pressures and temperatures for single shock, double shock, and multiple shock compression of liquid nitrogen provide a good match to the measured results over a broad range of *P*-*T* space. These calculations provide the first comparison of EOS developments with recently-measured *P*-*T* states under multiple shock compression. The present EOS developments are general and are expected to be useful for other liquids that have low pressure reference EOS information available.

I. INTRODUCTION

The response of liquid nitrogen (LN_2) at high pressures and high temperatures (HP-HT) has long been a subject of considerable scientific interest, due to its importance for understanding simple molecular liquids at extreme conditions, for planetary science and for chemical explosives technology. Experimental studies of LN_2 have been carried out primarily using shock wave compression to achieve HP-HT conditions. In these studies, pressure-volume (*P*-*v*) states have been determined for single shock[1-5] and double shock[4,5] loading; pressure-temperature (*P*-*T*) states for singly and doubly shocked LN_2 have been also been determined.[5-7] From previous measurements, it was inferred that LN_2 undergoes dissociation to atomic nitrogen for single shock loading above ~30 GPa.[3,5] For double shock loading, dissociation occurs at somewhat higher pressures[4-6] and leads to unusual features in the shock compression response.[4,5]

Theoretical studies have been undertaken for LN_2 to describe and understand the experimental findings indicated above. In particular, thermodynamic states for shocked LN_2 have been calculated using equation of state (EOS) developments for molecular nitrogen[8-12] and for mixtures of molecular and atomic nitrogen,[10-12] and also using density functional theory.[13] Although the EOS developments were all based on atomistic methods using pairwise potentials, they differed significantly in the level of agreement that they provided with the shock compression measurements[1-6] and the results were sensitive to the details of the pairwise potentials.[12]

To carry out numerical wave propagation simulations or thermochemical calculations, analytical EOS descriptions are advantageous. Previously, Belak and coworkers[9] used Monte Carlo methods with an intermolecular potential for N_2 to provide EOS points over a wide range of thermodynamic space. The calculated points were then fit using smooth functions to provide an analytical EOS formulation. However, because the calculated results were compared with experimental data at room temperature only, the quantitative accuracy of the EOS at HP-HT conditions is unknown. Using a somewhat different approach, Fried and Howard[12] used Chebyshev polynomials to provide an analytical approximation to the thermodynamic response arising from atomistic calculations using the exponential-six (exp-6) interatomic potential. Different parameterizations of the potential were used to describe N_2-N_2 interactions and N-N

interactions and mixing rules were defined to provide a description of LN_2 shocked below and above the dissociation threshold. The exp-6 potential parameters were adjusted to provide a best fit to available data from single- and double-shock experiments and static compression experiments.[12] Although the resulting EOS provided reasonable agreement with measured end states for shocked LN_2, its analytical expressions were based on a fairly complex system of fitting functions having large numbers of fitting parameters.[12] For many applications in shock wave physics, planetary science, and chemical explosives technology, a relatively simple, robust analytical EOS for LN_2 at HP-HT conditions is advantageous. The development of such an EOS was the objective of the present work.

For molecular nitrogen, as for many other fluids, an accurate reference EOS was developed previously by fitting a complex analytical function to a wide range of experimental data at relatively low pressures (up to ~2 GPa for N_2).[14] Although the complexity of the fitting function renders the EOS unsuitable for use at high pressures, where few experimental data for N_2 are available, the availability of a reference EOS at low pressures raises the question: Can an accurate low-pressure EOS, combined with data from shock compression experiments, be used to develop an analytical EOS that is accurate to high pressures and high temperatures? Here, we present EOS developments and calculations for shocked LN_2 that answer this question in the affirmative.

Recently, Raman spectroscopy was used[15] to measure temperatures for multiply-shocked LN_2, thus extending the range of pressure-temperature (*P*-*T*) space examined under dynamic compression. Because the measured *P*-*T* states for multiply-shocked LN_2 are significantly different from the Hugoniot curve (defined as the locus of end states attainable by single shock compression), they provide a more stringent test of the EOS developments than earlier measurements. Thus, to comprehensively examine the accuracy of our EOS developments, *P*-*T* states for single shock, double shock, and multiple shock loading were calculated and compared with measured values from available experimental studies on shocked LN_2.[5-7,15] We emphasize that our EOS developments are for molecular nitrogen only; dissociation of shocked LN_2 into atomic nitrogen is not addressed here.

The EOS developments for LN_2, including the incorporation of analytical models, are presented in Sec. II. In Sec. III, the calculated *P*-*T* states for LN_2 are compared with

experimental results from single, double, and multiple shock compression. A summary and conclusions are presented in Sec. IV.

II. EQUATION OF STATE DEVELOPMENT

The overall EOS development approach for LN_2 was based on that used previously for liquid nitromethane:[16] analytical expressions were developed for the specific heat at constant volume, c_v; the coefficient of thermal pressure, $\left(\partial P/\partial T\right)_v$; and the isothermal bulk modulus, B_T, as functions of temperature *T* and volume *v*. These three coefficients are sufficient to determine the Helmholtz potential $F\left(T,v\right)$ for the system, resulting in a complete EOS. To ensure thermodynamic consistency and to optimally use available data, appropriate thermodynamic relationships were employed in the development of the analytical models.

In addition to the reference EOS developed by Span, et al.[14] for LN_2 at low pressures (up to ~2 GPa), experimental Hugoniot data [1-5] and temperature measurements[5-7,15] are available for shocked LN_2. Therefore, to provide an EOS accurate to high pressures and high temperatures, analytical expressions for the above thermodynamic coefficients were developed using the following sequential approach: 1) c_v was determined by fitting to the calculated results from the Span, et al. EOS;[14] 2) $\left(\partial P/\partial T\right)_v$ was determined using thermodynamic relationships, Hugoniot data,[1-5] and temperature measurements for shocked LN_2;[5,6,15] 3) B_T was determined using thermodynamic relationships and temperature measurements for shocked LN_2.[5,6,15]

A. Specific heat model

Isochoric and isothermal values for the specific heat c_v, determined using the Span, et al. EOS,[14] are shown as the dashed curves in Figs. 1 and 2, respectively. These figures show that c_v

possesses a somewhat complex temperature dependence, together with significant volume dependence.

To describe the dependence of c_v on temperature and volume, we first note that the specific heat of LN_2 contains contributions from translational, rotational, vibrational, and electronic degrees of freedom. Because contributions from the electronic degrees of freedom are significant only at very high temperatures,[14] where dissociation of the nitrogen molecule has been previously inferred,[3-5] the electronic degrees of freedom were neglected in the developments presented here for molecular nitrogen. As in our previous work,[16] the vibrational contribution was determined using a single Einstein function. In keeping with our goal of developing an analytical EOS that will provide robust extrapolation to high pressures, the translational and rotational contributions were described using a constant term plus a second term having a linear dependence on the compression parameter $\mu = v_0/v - 1$ and a reciprocal square root dependence on temperature. Combining these different contributions leads to the following expression:

$$c_v(T,v) = R\left(C_0 + C_1 \frac{(C_2\mu + 1)}{\sqrt{T}} + C_3 \frac{x^2 e^x}{\left(e^x - 1\right)^2} \right), \qquad (1)$$

where $x = \theta/T$, θ is the Einstein temperature, C_0, C_1, C_2, and C_3 are constants and R is the ideal gas constant. Because θ is related to the frequency of the LN_2 internal vibration, it is volume dependent, in principle. However, the measured Raman frequency of LN_2 was previously shown to undergo only small changes (2% or less) in response to shock wave compression.[15] Parameter variation studies, carried out using Eq. (1), showed that calculated pressures and temperatures for shocked LN_2 are insensitive to 2% changes in θ. Therefore, θ was assumed constant in the EOS developments presented here.

Isochoric and isothermal values for c_v, determined using Eq. (1), are shown as the solid curves in Figs. 1 and 2, respectively. The parameters C_0, C_1, C_2, C_3 and θ used in these calculations are listed in Table I. The figures show that Eq. (1) provides a good match to the c_v values from the Span, et al. EOS over a wide range of temperatures and volumes.

$c_v(T,v)$ curves along the Hugoniot and along the isentrope, calculated using Eq. (1) (solid curve), are shown in Fig. 3. Also shown are corresponding calculations using the Span, et al. EOS (dashed curve).[14] The results in Fig. 3 show that $c_v(T,v)$ calculations using the two different EOS developments match reasonably well along the Hugoniot. However, calculations along the isentrope show different trends and diverge considerably at larger compressions. Because the accuracy of the Span, et al. EOS at high pressures is uncertain, the divergence of the two calculations along the isentrope is not a significant concern.

B. Determination of $(\partial P/\partial T)_v$

The determination of $(\partial P/\partial T)_v$ begins with the thermodynamic identity

$$\frac{\partial}{\partial T}\left(\frac{\partial P}{\partial T}\right)_v = \frac{1}{T}\frac{\partial c_v}{\partial v} \ . \tag{2}$$

Substituting Eq. (1) into (2), performing the derivative on the right hand side, and integrating with respect to *T* yields

$$\left(\frac{\partial P}{\partial T}\right)_v = \left(\frac{\partial P}{\partial T}\right)_v\Bigg|_{T=T_0} + 2RC_1C_2\left(\frac{v_0}{v^2}\right)\left(\frac{1}{\sqrt{T}}-\frac{1}{\sqrt{T_0}}\right). \tag{3}$$

where $(\partial P/\partial T)_v\big|_{T=T_0}$ is evaluated along the 77 K isotherm and the constants C_1, C_2, and R are defined in Eq. (1). $(\partial P/\partial T)_v\big|_{T=T_0}$ was determined by integrating Eq. (3) with respect to *T* and solving to obtain

$$\left(\frac{\partial P}{\partial T}\right)_v\Bigg|_{T=T_0} = \frac{P(T_H,v)-P(T_0,v)}{T_H-T_0} - 2RC_1C_2\left(\frac{v_0}{v^2}\right)\left(\frac{2\left(\sqrt{T_H}-\sqrt{T_0}\right)}{T_H-T_0}-\frac{1}{\sqrt{T_0}}\right), \tag{4}$$

where $P(T_H, v)$ and $P(T_0, v)$ are the pressures on the Hugoniot curve and on the liquid isotherm, respectively.

To evaluate Eq. (4), *P*-*v* Hugoniot and isothermal compression curves for LN_2 are needed. For the Hugoniot curve, shock compression data[1-5] for LN_2 were fit using the expression proposed by Woolfolk, et al.,[17]

$$\frac{U_s}{c_0} = a_1 + (1 - a_1)\exp\left[-a_3 u_p / c_0\right] + a_2 \frac{u_p}{c_0} \ , \tag{5}$$

where U_s is the shock wave velocity, u_p is the particle (mass) velocity, c_0 is the acoustic velocity at ambient pressure and temperature (~77 K) for LN_2, and a_1, a_2, and a_3 are constants determined from the fit. The fit to the Hugoniot data is shown in Fig. 4, together with the Hugoniot curve calculated using the Span, et al. EOS.[14] The good agreement between the Span, et al. Hugoniot and the measured results is not surprising because Hugoniot data[1,3] were used by Span, et al. in their EOS development. The parameter values in Eq. (5), determined from the fit, are shown in Table I.

Because LN_2 freezes at very low pressure on the T = 77 K isotherm, measured isothermal compression data for the liquid phase are not available at high pressures. Therefore, to enable evaluation of Eq. (4), the Vinet equation[18,19]

$$P(v) = \frac{3B_0\left(1 - X\right)}{X^2}\exp\left[\frac{3}{2}\left(B' - 1\right)\left(1 - X\right)\right] \ ; \quad X = \left(\frac{v}{v_0}\right)^{1/3} , \tag{6}$$

was used to construct an isothermal compression curve for supercooled LN_2. The bulk modulus in the initial state, B_0, was determined using the Span, et al. EOS.[14] However, in the absence of experimental data to determine the B' parameter in Eq. (6), B' was adjusted to provide the best match to measured *P*-*T* states (see Sec. II D).

$\left(\partial P/\partial T\right)_v\big|_{T=T_0}$ was determined, together with the Hugoniot temperature T_H, by a simultaneous solution involving Eq. (1) and Eqs. (3) – (6), together with general thermodynamic

relationships. The resulting values for $\left(\partial P/\partial T\right)_v\Big|_{T=T_0}$ along the 77 K isotherm are shown in Fig. 5 (black dotted curve). Fitting the $\left(\partial P/\partial T\right)_v\Big|_{T=T_0}$ values with a polynomial (black solid curve in Fig. 5) and incorporating the polynomial in Eq. (3) provides an analytical expression for $\left(\partial P/\partial T\right)_v$ as a function of temperature and volume.

Figure 5 shows $\left(\partial P/\partial T\right)_v$ along the Hugoniot curve and along the isentrope, as calculated using Eq. (3). As shown in Fig. 5, $\left(\partial P/\partial T\right)_v$ along the Hugoniot curve matches reasonably well with corresponding calculations using the Span, et al. EOS.[14] Figure 5 also shows that, at larger compressions, the calculated results for $\left(\partial P/\partial T\right)_v$ on the isentrope diverge somewhat from the corresponding calculations using the Span, et al. EOS, consistent with the divergence observed for c_v in Fig. 3.

To further examine the behavior of our EOS developments at high pressures and high temperatures, Eqs. (1) and (3) were used to determine the Grüneisen parameter Γ along the Hugoniot and the isentrope, using the thermodynamic identity

$$\Gamma = \frac{v}{c_v}\left(\frac{\partial P}{\partial T}\right)_v \quad . \tag{7}$$

The results, presented in Fig. 6, show that Γ along the Hugoniot is in reasonable agreement with corresponding calculations using the Span, et al. EOS.[14] However, at larger compressions, the calculated results for Γ on the isentrope diverge somewhat from results calculated using the Span, et al. EOS, consistent with the divergence observed for c_v in Fig. 3 and for $\left(\partial P/\partial T\right)_v$ in Fig. 5.

C. Determination of B_T

Determination of B_T begins with the thermodynamic identity

$$\frac{\partial B_T}{\partial T} = -v\frac{\partial}{\partial v}\left(\frac{\partial P}{\partial T}\right)_v . \tag{8}$$

Substituting Eq. (3) into (8), performing the derivative on the right hand side, and integrating with respect to *T* yields

$$B_T(T,v) = B_T(T_0,v) - v(T-T_0)\frac{\partial}{\partial v}\left(\frac{\partial P}{\partial T}\right)_v\Bigg|_{T=T_0} + 4RC_1C_2\left(\frac{v_0}{v^2}\right)\left[2\left(\sqrt{T}-\sqrt{T_0}\right) - \frac{(T-T_0)}{\sqrt{T_0}}\right]. \tag{9}$$

In Eq. (9), $B_T(T_0,v)$ was determined using Eq. (6), $(\partial P/\partial T)_v\big|_{T=T_0}$ was determined using Eq. (4), and C_1, C_2, and R were defined in Eq. (1).

D. Determination of the B' parameter

With one exception, the EOS model parameters discussed above were determined directly from experimental data or by comparison with the low pressure EOS of Span, et al.[14] The remaining parameter, B' in Eq. (6), was adjusted to provide the best match between pressure-temperature (*P*-*T*) states calculated using the EOS developments from Sec. II A – C and the available measured *P*-*T* states for shocked LN_2;[5,6,15] the resulting B' value is shown in Table I. The calculated *P*-*T* states are presented next and are compared to experimental results.

III. PRESSURE-TEMPERATURE STATES FOR SHOCKED LIQUID NITROGEN

Measured pressure-temperature states for single shock,[5-7] double shock,[6] and multiple shock[15] compression of LN_2 are shown as the open symbols in Fig. 7. The states shown are those for which the peak pressures and temperatures are below the reported dissociation thresholds for single shock and double shock loading.[5,6] The measured states from Ref. 6 are

shown without error bars because quantified experimental uncertainties were not provided; a rough estimate of the uncertainty can be inferred from the scatter in the data. In addition, we note that the peak pressures for the double shock states in Ref. 6 were not measured, but instead were calculated using an EOS developed previously.[8] Also, we note that the measured temperatures for single shock states from Ref. 7 (not shown) are systematically lower, compared to those from Refs. 5 and 6 (red open squares). Due to insufficient information regarding the experimental methods, the reliability of the results from Ref. 7 is difficult to ascertain. Therefore, the results from Ref. 7 are not discussed further.

As expected for undissociated molecular N_2, Fig. 7 shows that the measured temperatures for each loading condition increase monotonically with increasing peak pressure. In addition, the peak temperatures for double shock loading and for multiple shock loading are significantly lower than for single shock loading, again as expected. Thus, the measured shocked states span a large range of pressures and temperatures.

P-*T* states for single shock, double shock, and multiple shock compression of LN_2, calculated using the EOS developments from Sec. II, are shown as the filled symbols in Fig. 7. Overall, the calculated *P*-*T* states are in good agreement with the measured states; several of the calculated multiple shock states lie slightly outside the error bars of the measured states.

Also shown in Fig. 7 are Hugoniot and isentropic compression curves, calculated using the EOS presented here, together with those calculated using the Span, et al. EOS.[14] The isentropic compression curves calculated using these two EOS developments are in reasonable agreement. However, although the $U_s - u_p$ Hugoniot curves for the EOS presented here and for the Span, et al. EOS are a close match (Fig. 4), the *P*-*T* states along the Hugoniot curves deviate significantly with increasing pressure in Fig. 7. These results are consistent with previous conclusions[16,20] that temperature measurements are important in discriminating between different EOS developments. In addition, the *P*-*T* states along the Hugoniot calculated using the Span, et al. EOS lie well outside the error bars for most of the measured single shock states from Refs. 5 and 6. This finding demonstrates the importance of using analytical models that are robust and theoretically sound to guide extrapolations of low pressure EOS to HP-HT conditions.

The large range of pressures and temperatures spanned by the experimental results provides a strong test of EOS developments. In particular, the recently measured multiple shock

states[15] are far from the Hugoniot curve, which is often used to validate EOS developments.[8,10-12] Therefore, the good overall match of the present calculations to the measured results in Fig. 7 – spanning a wide range of *P*-*T* states – suggests that our EOS developments provide a good description of the response of shocked LN_2 at high pressures and high temperatures. In addition, we note that all but one of the parameters in our EOS models were determined by comparison with $U_s - u_p$ Hugoniot data or with the low pressure EOS of Span, et al.[14] The good agreement of the calculated results with the measured *P*-*T* states in Fig. 7 was obtained by adjusting a single free parameter, namely the B' parameter in Eq. (6). In contrast, multiple free parameters were used in many of the previous EOS developments.[10-12]

Although the EOS developments presented here provide a good match to experimental data for shocked LN_2 over a wide range of pressures and temperatures, we note that Eq. (4) establishes the Hugoniot curve as an upper bound on the expected region of validity for the present EOS developments. In addition, because the isothermal compression curve defined by Eq. (6) is associated with supercooled fluid N_2, the melt curve for N_2 provides a lower bound on the region of EOS validity. Extrapolation of our EOS models to *P*-*V*-*T* states beyond these bounds should be undertaken with caution.

SUMMARY AND CONCLUSIONS

A relatively simple analytical EOS for shocked liquid nitrogen (LN_2) was developed based on a theoretical framework used previously for liquid nitromethane.[16] Parameters for the analytical models were determined by comparison with the low pressure reference EOS of Span, et al.[14] and with experimental data for shocked LN_2.[1-6,15] This approach is in contrast to previous EOS developments for shocked LN_2, which focused on the use of pairwise potentials in atomistic calculations.[8-12]

Pressure-temperature (*P*-*T*) states for single shock, double shock, and multiple shock compression of LN_2, calculated using the EOS presented here, showed good overall agreement with measured states.[5,6,15] The good match to the measured *P*-*T* states was obtained using only a single adjustable parameter, in contrast to the multiple free parameters used in many of the

previous EOS developments.[10-12] Direct extrapolation of the Span, et al. EOS[14] resulted in a *P-T* Hugoniot curve that was well outside the error bars of the measured single shock states, showing that extrapolations of low pressure EOS developments to high pressures and high temperatures need to be guided by robust, theoretically sound analytical models. The results presented here are consistent with the previous conclusion[16,20] that temperature measurements are important in discriminating between different EOS developments.

The calculations presented here provide the first comparison of EOS developments with recently-measured multiple shock *P-T* states for LN_2.[15] Because the measured multiple shock states are far from the single shock Hugoniot curve in the *P-T* plane, they provide a strong test of EOS developments. Hence, the good overall match between the present calculations and the measured *P-T* states suggests that our EOS developments provide a good description of LN_2 at high pressures and high temperatures.

In addition to liquid nitrogen, low pressure reference equations of state are available for a variety of different liquids. Therefore, our approach for using analytical EOS models to extrapolate low pressure EOS developments to high pressure-high temperature conditions will likely be useful for modeling the response of other shocked liquids, in addition to nitrogen.

ACKNOWLEDGEMENTS

This work was supported by the Department of Energy/NNSA under Cooperative Agreement No. DE-NA0002007.

References

[1] V. N. Zubarev and G. S. Telegin, Sov. Phys. Dokl. **7**, 34 (1962).

[2] R. D. Dick, J. Chem. Phys. **52**, 6021 (1970).

[3] W. J. Nellis and A. C. Mitchell, J. Chem. Phys. **73**, 6137 (1980).

[4] W. J. Nellis, N. C. Holmes, A. C. Mitchell, and M. van Thiel, Phys. Rev. Lett. **53**, 1661 (1984).

[5] W. J. Nellis, H. B. Radousky, D. C. Hamilton, A. C. Mitchell, N. C. Holmes, K. B. Christianson, and M. van Thiel, J. Chem. Phys. **94**, 2244 (1991).

[6] D. S. Moore, S. C. Schmidt, M. S. Shaw, and J. D. Johnson, J. Chem. Phys. **90**, 1368 (1989).

[7] I. M. Voskoboinikov, M. F. Gogulya, and Yu. A. Dolgoborodov, Sov. Phys. Dokl. **24**, 375 (1979).

[8] J. D. Johnson, M. S. Shaw, and B. L. Holian, J. Chem. Phys. **80**, 1279 (1984).

[9] J. Belak, R. D. Etters, and R. LeSar, J. Chem. Phys. **89**, 1625 (1988).

[10] M. Ross, J. Chem. Phys. **86**, 7110 (1987).

[11] M. Van Thiel and F. H. Ree, J. Chem. Phys. **104**, 5019 (1996).

[12] L. E. Fried and W. M. Howard, J. Chem. Phys. **109**, 7338 (1998).

[13] S. Mazevet, J. D. Johnson, J. D. Kress, L. A. Collins, and P. Blottiau, Phys. Rev. B 65, 014204 (2002).

[14] R. Span, E. W. Lemmon, R. T. Jacobsen, W. Wagner, and A. Yokozeki, J. Phys. Chem. Ref. Data **29**, 1361 (2000).

[15] D. Lacina and Y. M. Gupta, J. Chem. Phys. **141**, 084503 (2014).

[16] J. M. Winey, G. E. Duvall, M. D. Knudson, and Y. M. Gupta, J. Chem. Phys. **113**, 7492 (2000).

[17] R. W. Woolfolk, M. Cowperthwaite, and R. Shaw, Thermochim. Acta **5**, 409 (1973).

[18] P. Vinet, J. Ferrante, J. R. Smith and J. H. Rose, J. Phys. C: Solid State Phys. **19**, L467 (1986).

[19] P. Vinet, J. R. Smith, J. Ferrante and J. H. Rose, Phys. Rev. B **35**, 1945 (1987).

[20] J. M. Winey, Y. A. Gruzdkov, Z. A. Dreger, B. J. Jensen, and Y. M. Gupta, J. Appl. Phys. **91**, 5650 (2002).

Table I. Parameters used in Eqs. (1), (5), and (6).

Parameter	Value
C_0	2.84
C_1	6.00 $K^{1/2}$
C_2	7.50
C_3	0.94
θ	3364 K
a_1	2.347
a_2	1.287
a_3	0.80
B_0	0.3116 GPa
B'	8.1

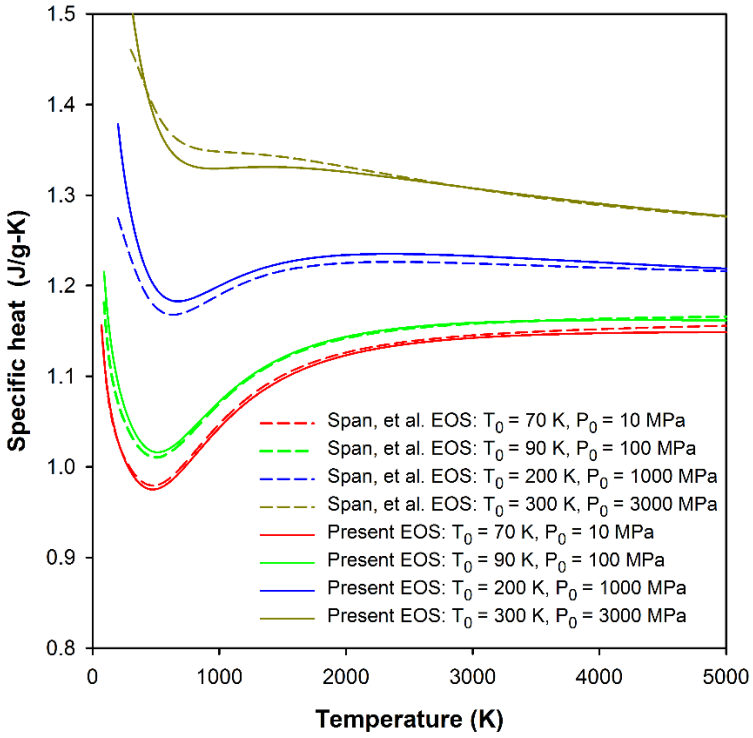

Figure 1. Specific heat c_v versus temperature along several isochores. The solid and dashed lines are calculations using Eq. (1) and the Span, et al. EOS (Ref. 14), respectively. T_0 and P_0 are the initial temperature and pressure for each isochore.

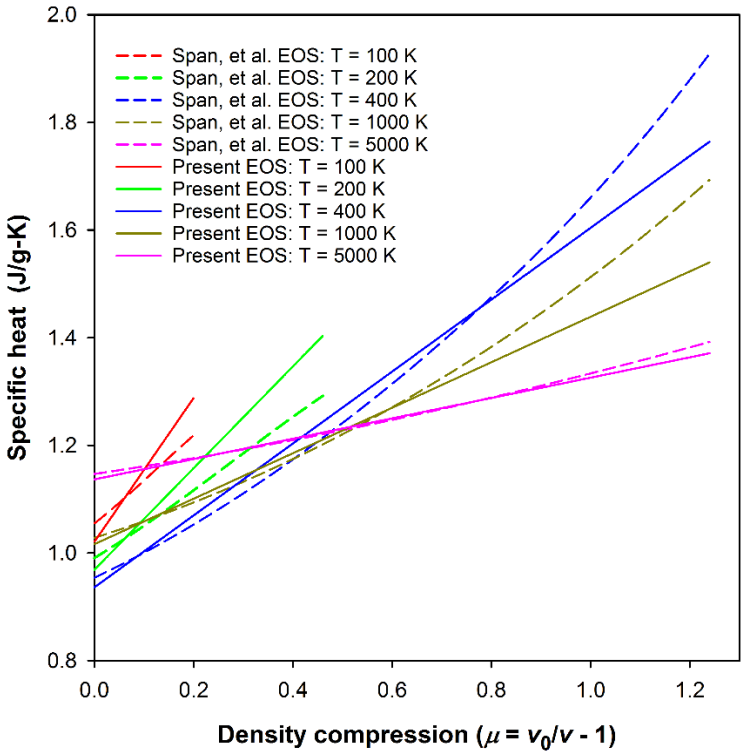

Figure 2. Specific heat c_v versus density compression along several isotherms. The solid and dashed lines are calculations using Eq. (1) and the Span, et al. EOS (Ref. 14), respectively.

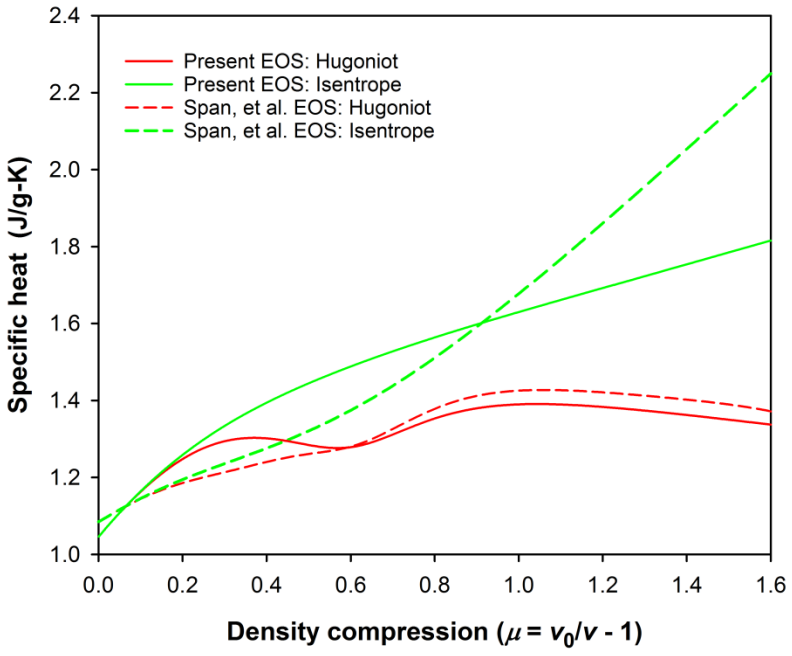

Figure 3. Specific heat c_v versus density compression for LN_2. The red and green solid curves are c_v along the Hugoniot and isentrope, respectively, calculated using the present EOS. The red and green dashed curves are c_v along the Hugoniot and isentrope, respectively, calculated using the EOS from Ref. 14.

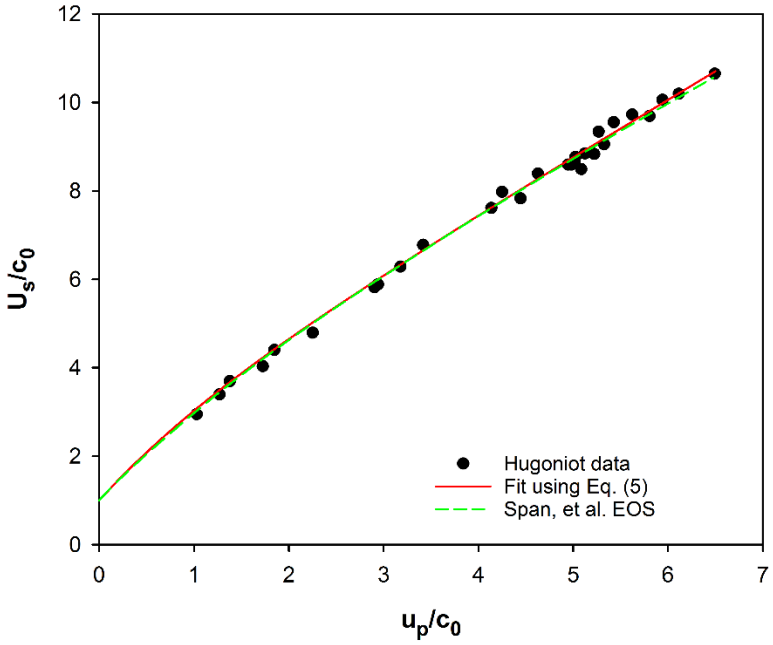

Figure 4. Locus of shock compression end states (Hugoniot curve) for liquid nitrogen. U_S is shock velocity, u_p is particle velocity, and c_0 is the sound velocity of LN_2 at 77 K. The solid circles are measured results from Refs. 1-3. The solid red curve is a fit using Eq. (5) and the dashed green curve is a calculation using the EOS from Ref. 14.

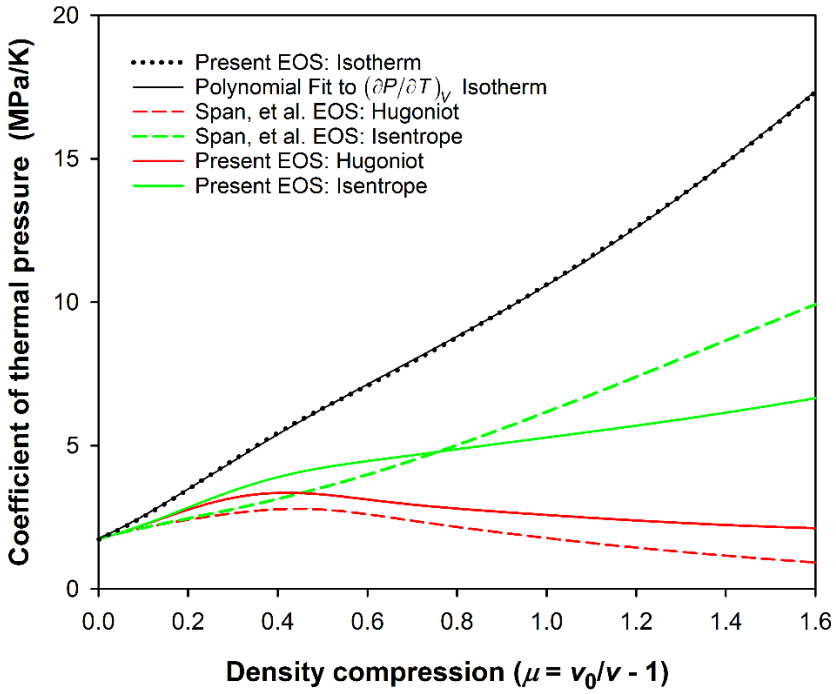

Figure 5. Coefficient of thermal pressure $\left(\partial P/\partial T\right)_V$ versus density compression for LN_2. The black dotted curve is $\left(\partial P/\partial T\right)_V$ along the 77 K isotherm. The black solid curve is a polynomial fit to $\left(\partial P/\partial T\right)_V$ along the 77 K isotherm. The red and green solid curves are $\left(\partial P/\partial T\right)_V$ along the Hugoniot and isentrope, respectively, calculated using the present EOS. The red and green dashed curves are $\left(\partial P/\partial T\right)_V$ along the Hugoniot and isentrope, respectively, calculated using the EOS from Ref. 14.

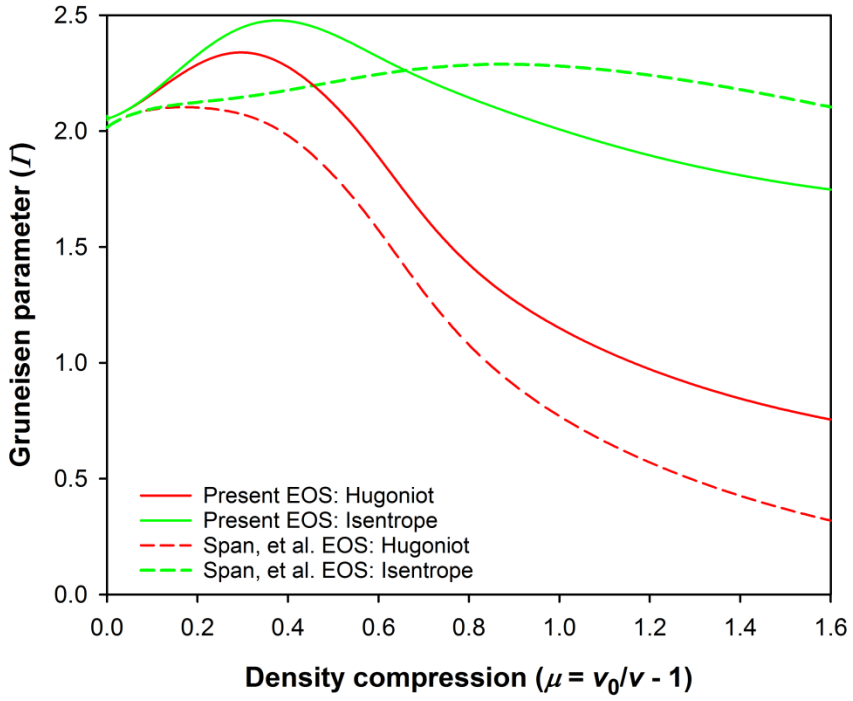

Figure 6. Grüneisen parameter Γ versus density compression for LN_2. The red and green solid curves are Γ along the Hugoniot and isentrope, respectively, calculated using the present EOS. The red and green dashed curves are Γ along the Hugoniot and isentrope, respectively, calculated using the EOS from Ref. 14.

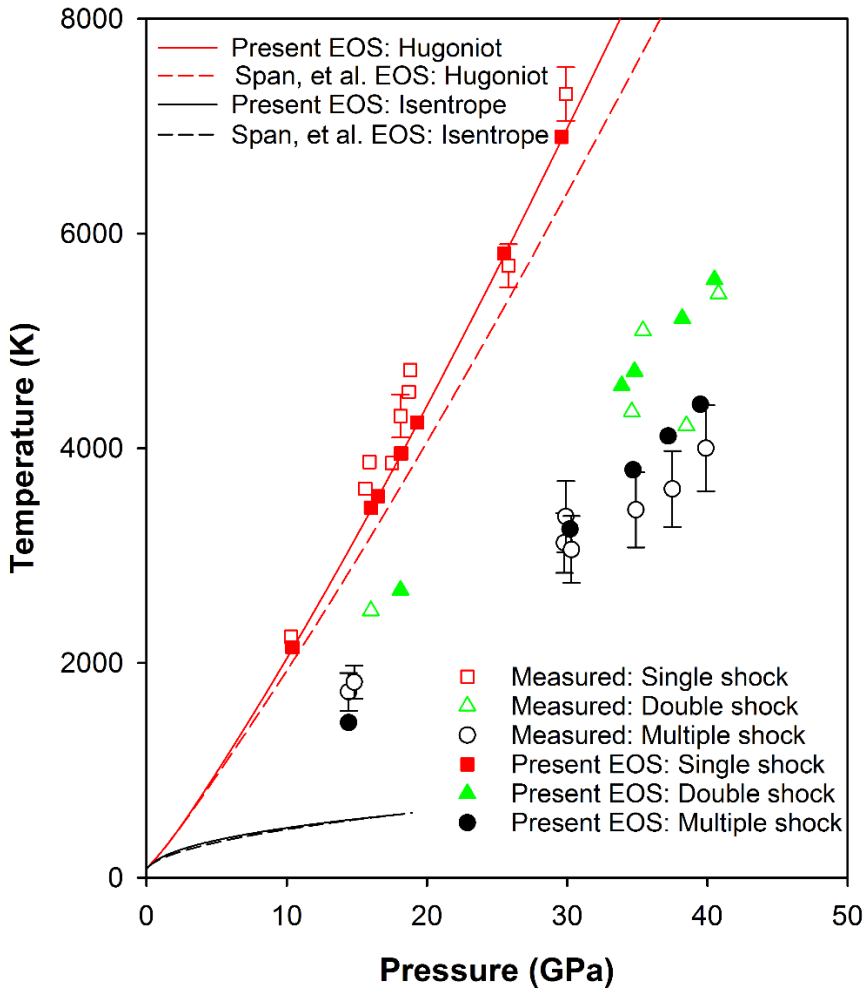

Figure 7. Temperature-pressure states for dynamic compression of LN_2. The open symbols are measured peak states for single shock (red squares: Refs. 5, 6), double shock (green triangles: Ref. 6), and stepwise loading (black circles: Ref. 15). The corresponding filled symbols and the solid curves are calculations using the EOS presented here. The dashed curves are calculations using the EOS from Ref. 14. Uncertainty bounds were not available for the measured states (single shock and double shock) from Ref. 6.